A Photon Echo Peak Shift Study of Liquid Water†

Jens Stenger,‡ Dorte Madsen,§,‡ Peter Hamm,*,||,‡ Erik T. J. Nibbering,‡ and Thomas Elsaesser‡

Max-Born-Institut für Nichtlineare Optik und Kurzzeitspektroskopie, Max-Born-Strasse 2A, D-12489 Berlin, Germany, and Department of Chemistry, Aarhus University, Langelandsgade 140, 8000 Aarhus C, Denmark

Received: August 8, 2001; In Final Form: October 31, 2001

The first photon echo peak shift study of liquid water is presented. Spectral diffusion within the OH stretching absorption band of HDO in D_2O takes place on many time scales with a slow component on the order of 5−15 ps. This indicates that fluctuations of local structure of the hydrogen bond network in liquid water are relatively long-lived. Vibrational relaxation of the excited state populates a state which is spectroscopically different from the initial ground state. This leads to an strong enhancement of the peak shift and allows spectral diffusion to be measured for delay times beyond the limit determined by the population relaxation time T_1. The observed signals are discussed with the help of model calculations.

1. Introduction

Determination of the structural fluctuations of the hydrogen bond network in liquid water is crucial for the understanding of its outstanding physical and chemical properties. These fluctuations take place on ultrafast time scales and are reflected in the stochastic behavior of transition frequencies between vibrational energy levels that are sensitive to hydrogen bonding. It is well-known that the OH stretching vibration probes the local microscopic structure because its frequency shift due to hydrogen bonding scales roughly linearly with the OH···O distance.[1] Hence, the correlation function of the fluctuations of the transition frequency, which is an experimentally accessible quantity, is of great interest because it gives direct information about structural fluctuations.

The structural dynamics of liquid water have been addressed recently by ultrafast vibrational spectroscopy. A 700 fs spectral diffusion process has been reported which was observed in hole-burning experiments on the OH stretch absorption band of HDO in D_2O.[2] In these measurements infrared laser pulses of 150 fs duration have been used to monitor the spectral shift of the transient spectrum over time. Independent of excitation wavelength the first moment of the transient spectrum moves to the center of the absorption band. The data have been fit using a frequency fluctuation correlation function which decays monoexponentially with a correlation time of 700 fs. However, we have determined that a major part of the broad absorption band (120 out of 235 cm^{-1} fwhm) is due to homogeneous broadening[3] and that therefore a dominating part of the frequency fluctuation correlation function decays on an ultrafast sub-100 fs time scale. A water model with three major structural components has been proposed[4] on the basis of hole-burning experiments with 2 ps pump pulses and 1 ps probe pulses. The results are interpreted by structural cross relaxation between the different constituents with a time constant of 1 ps. On the other hand, probing orientational dynamics by anisotropy decay measurements suggests a mixture model for which only two species of local structures or hydrogen bond lifetimes exist.[5] Here, the authors assume that an observed time constant of 13 ps in the orientational relaxation of excited OH dipoles might be connected to a process involving the breaking of a hydrogen bond and therefore also structural relaxation.

Though such studies have provided substantial insight into the structural dynamics of water, the full correlation function of the transition frequency remains unknown. Three-pulse photon echo measurements,[7,8] a technique recently also demonstrated in the midinfrared spectral range,[6] have the potential to reveal this information. The essential quantity from such an experiment is the so-called three-pulse photon echo peak shift (3PEPS), whose evolution under increasing population time T has been found to be a highly informative quantity. It has been shown[7,8] that for a simple two-level system this quantity directly resembles the frequency correlation function of the transition under investigation. The same is true for simple vibrational three-level systems,[6] consisting of $\nu = 0$, $\nu = 1$, and $\nu = 2$ states.

In this contribution we present 3PEPS measurements on the OH stretching absorption band of HDO in D_2O. Data for different spectral positions within this band display a fast decay of the peak shift within the first 500 fs. At longer delays, we observe a pronounced rise of peak shift in the red part of the spectrum, reaching a maximum after 2 ps and decaying subsequently within several picoseconds. This behavior cannot be explained within simple two- or three-level models. The coupling of the OH stretching mode to intermolecular degrees of freedom of the hydrogen bond network of water, which are excited and eventually heated upon dissipation of the energy initially pumped into the OH vibration, has a strong effect on the peak shift data and is taken into account by a more sophisticated energy level scheme. For this case the peak shift does not directly resemble the frequency fluctuation correlation function. Nevertheless, the 3PEPS results still do uncover the dynamic properties of the transition under study. With the help of numerical model calculations we conclude that spectral diffusion in water cannot be described only by a single-

† Part of the special issue "Noboru Mataga Festschrift".

* To whom correspondence should be addressed.
‡ Max-Born-Institut für Nichtlineare Optik und Kurzzeitspektroskopie.
§ Department of Chemistry.
|| New address: Physikalisch Chemisches Institut, Universität Zürich, Winterthurerstr. 190, CH-8057 Zürich, Switzerland.

10.1021/jp013104k CCC: $22.00
Published on Web 01/29/2002

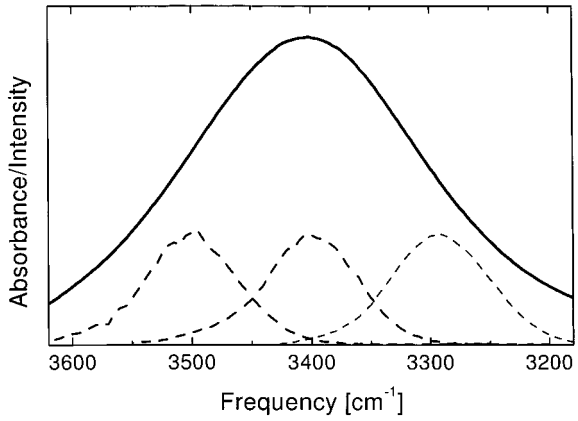

Figure 1. Absorption spectrum of the OH stretch vibration of HDO in D_2O corrected for D_2O background (solid) and the power spectra of the laser pulses (dashed).

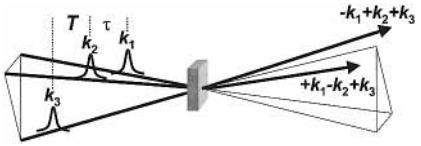

Figure 2. Schematic configuration of the four-wave-mixing experiment. τ describes the temporal delay between the first and the second pulse with wave vectors k_1 and k_2. T is the time between second and third pulse (with wave vector k_3). This geometry allows the spatial separation of the third-order polarization generated in the $-k_1 + k_2 + k_3$ and the $+k_1 - k_2 + k_3$ phase matching directions.

exponential process, as deduced from the spectral hole-burning experiments,[2] but takes place on many time scales including a slower component on the order of 5−15 ps.

2. Experimental Section

Since a stimulated photon echo signal scales with the third power of the pulse energy (see below), it is crucial to have a stable high power light source available. To generate intense midinfrared laser pulses in the femtosecond regime we use optical parametric amplification. Pulses at 800 nm with an energy of 300 μJ and a duration of 90 fs from an amplified laser system based on Ti:sapphire are converted in a $KTiOPO_4$ crystal in two stages. The first stage is seeded by a single filament white light continuum and pumped by 3 μJ at 800 nm. In the second stage pumping with 200 μJ yields 150 fs mid infrared pulses with an energy of 3−5 μJ. They are tunable between 3000 and 3600 cm^{-1} while the energy varies from 5 μJ at low frequencies to 3 μJ at high frequencies. The spectra of the laser pulses used in this work and their position with respect to the OH stretching absorption band of HDO in D_2O are shown in Figure 1.

The measurement principle of the photon echo peak shift experiment is the following: The laser pulse tuned to the transition frequency is split into three parts with wave vectors k_1, k_2, and k_3, the wave vectors being of parallel polarization and approximately the same energy. These three beams are then focused onto the sample in the so-called box configuration (focal diameter of ~80μm), which allows the spatial separation of the third-order polarization in the phase matching directions $-k_1 + k_2 + k_3$ and $+k_1 - k_2 + k_3$ (see Figure 2). In both directions the four wave mixing signals are recorded simultaneously by two InSb detectors which integrate the light intensity over time. The pulse delay between the first two pulses k_1 and k_2 is conventionally called coherence time τ (which is defined as positive when k_1 arrives before k_2), while the period between

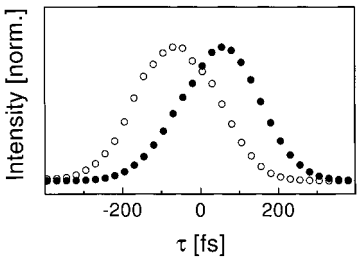

Figure 3. Integrated photon echo signals in liquid water for $T = 0$ fs as a function of coherence time τ. Solid symbols represent the signal in the $-k_1 + k_2 + k_3$ direction, while open symbols are used for the data taken in the $+k_1 - k_2 + k_3$ direction.

the pulse which arrives as the second pulse at the sample and the third pulse is referred to as population time T (which is positive). During the first time period τ, the system evolves in an (off-diagonal) coherence state, while it evolves in a (diagonal) population state during the second time period T. Both time periods are varied by computer controlled delay stages. Typical stimulated photon echo signals for one population time T are shown in Figure 3. The signals in the two phase matching directions are mirror images of one another and therefore the value of half the distance between the peaks can be extracted very accurately. This quantity is called the "peak shift", which is the essential property deduced from the experiment. Measuring the peak shift up to a delay time of 100 ps (where it is expected to be zero) indicates that it is subject to a systematic error of ≈3 fs, a phenomenon which has been observed before.[9] In addition, we report the "transient grating" decay, which is the four wave mixing signal as a function of population time T recorded for the coherence time τ set to zero.

The sample consists of HDO dissolved in D_2O so that the OH stretching absorption band of HDO reaches an optical density of 0.4 at 3400 cm^{-1} which corresponds to a concentration of 0.2M. This concentration has been shown to be small enough so that the O−H stretch modes can be regarded as isolated oscillators.[10] The liquid is held at 300K between two CaF_2 windows with a spacing of 300 μm and is rapidly circulated to avoid accumulation and heating effects.

3. Results

The experimental peak shift and transient grating signals are shown as a function of population time T in Figure 4 for the three spectral positions. For all wavelengths the peak shift at $T = 0$ has a value of around 50 fs indicating the presence of inhomogeneity in the absorption band. Within the first 200 fs of population time T the shift decays to about 20 fs. After 500 fs the behavior then shows a strong spectral dependence. In the center and in the blue wing of the ν_{OH} absorption band the signals stay constant at around 10−20 fs. However, on the red side of the band at 3300 cm^{-1} the peak shift rises again strongly starting at ~1 ps. At about $T = 2$ ps it reaches a maximum value of almost 50 fs followed by a decay down to 10 fs at $T = 4$ ps. The higher noise of the data on the blue side of the absorption line is due to the lower energy of the pulses generated for that wavelength.

The three normalized transient grating traces show for short times T a decay behavior close to exponential. The time constant is close to 300 fs suggesting a population relaxation on the order of 600 fs. However, here we use a parallel geometry of polarizations of the light pulses and therefore the measurement is sensitive to rotational diffusion. This is the reason T_1 appears somewhat faster than the true population relaxation time $T_1 =$ 700 fs measured in pump/probe experiments under magic

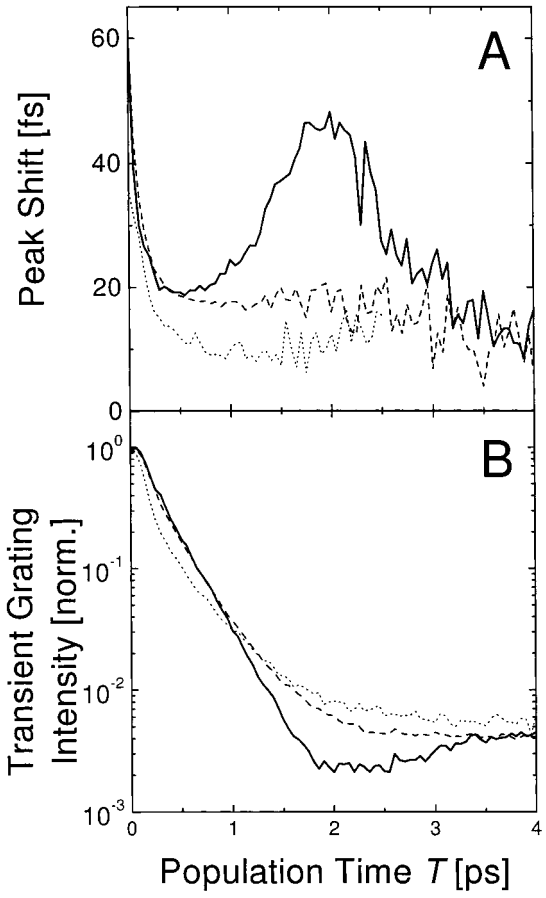

Figure 4. (A) Experimental three-pulse photon echo peak shift data for laser pulses centered at 3300 cm^{-1} (solid), 3400 cm^{-1}(dashed), and 3500 cm^{-1} (dotted). For the trace at 3500 cm^{-1} the data could be only collected up to $T = 2.5$ ps because of the smaller output power of the OPA at this wavelength (see Experimental Section). (B) The experimental normalized transient grating signal ($\tau = 0$) for the same spectral positions (labeling as in (A)).

angle.[5,11] After 1 ps, the transient grating signals flatten for 3500 and 3400 cm^{-1} to reach a small constant value ($\sim 4 \times 10^{-3}$) for long delay times. In the red at 3300 cm^{-1} the intensity has a dip at around 2 ps and rises again afterward to lead as well to a constant nonzero value for long delay times. We have observed this constant level in the transient grating signal for delay times up to 100 ps.

It has been verified that, within signal-to-noise, the peak shift data and the shape of the normalized transient grating signals are independent of the pulse energy which was varied by up to a factor of 5. Thus, artifacts from higher order nonlinearities can be excluded.

4. Theory

It has been shown that the peak shift measurement directly resembles the frequency fluctuation correlation function of the transition under investigation in simple two- and three-level systems.[6−8] In view of that work, the dramatic rise in the peak shift for the red part of the absorption band might seem surprising at a first sight. If this rise would directly reflect the frequency fluctuation correlation function, one would have to assume the existence of a low frequency, underdamped mode coupled to the OH stretching vibration. The exciting light pulse would coherently excite this mode and one would interpret the rise of the photon echo peak shift as a damped oscillation with a period on the order of 2 ps (frequency 500 GHz). However,

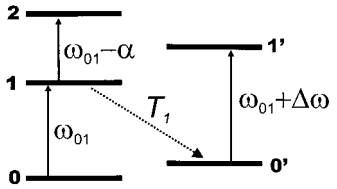

Figure 5. Energy level scheme for the hydrogen bonded OH stretching oscillator. The transition frequency from $\nu = 1$ to $\nu = 2$ is anharmonically shifted to the red by $\alpha = 270$ cm^{-1} [21] with respect to the $\nu = 0$ to $\nu = 1$ transition frequency ω_{01}. The population decay to a "hot" ground state $\nu = 0'$ introduces a transition from $\nu = 0'$ to $\nu = 1'$which is blue shifted by $\Delta\omega = 20$ cm^{-1} (see text) with respect to ω_{01}.

the existence of such a mode can be excluded from what we know from linear dielectric spectroscopy of water in that frequency range.[12]

Yang et al.[13] have shown that for optical echoes at very low temperatures the imaginary parts of the response functions of different Liouville space pathways can interfere in such a way that it produces such a rise in the peak shift. However, this situation does not apply here because all measurements were taken at room temperature. Nevertheless, a similar signal is predicted for reactive systems,[13] such as that for the energy transfer system LHC-II at room temperature.[14]

The excitation of the OH stretching mode in water initiates a sequence of fast relaxation steps[15] and returns to a state spectroscopically different from the original ground state:[18] The energy dissipated after vibrational relaxation heats the bulk sample. As the hydrogen bond potential is anharmonic, heating leads to a weakening of the hydrogen bonds which eventually results in an observable blue shift of the OH absorption band (see Figure 5). In that sense, the system might be viewed as a reactive system and the peak shift evolution is qualitatively similar to the mentioned work of Fleming and co-workers, even though the details of the underlying physical process are very different.

Nonlinear optical experiments, such as the three-pulse photon echo, are usually described with the help of a set of nonlinear response functions, one for each Liouville pathway (i.e., Feynman diagram, see Figure 6). The methodology has initially been developed to describe nonlinear spectroscopy of optical two-level systems.[20] The "standard" two-level diagrams are R_1 and R_5, which describe the contribution of the hole (i.e., the bleach), and R_2 and R_6, which describe the contribution of the excited state (i.e., stimulated emission). Both the bleach and stimulated emission contribute equally to the total signal. It is generally accepted that vibrational relaxation into the ground state can be considered by weighting the corresponding response functions with a phenomenological factor $\exp(-T/T_1)$,[6] which does not affect the peak shift but only reduces the intensity of the signal. This approach assumes that the bleach signal disappears simultaneously with the decay of the simulated emission signal. However, we see from the transient grating signal, which decays monoexponentially only up to $\approx$1.5 ps, that this simplifying approach is not appropriate for the description of the nonlinear response of water. Interestingly, the rise of the peak shift data appears at about the same delay time T, when the transient grating signal starts to deviate from a simple monoexponential decay.

The crucial point is that the excited molecules relax into a ground state which is spectroscopically different from the initial excited state. After a complicated and fast sequence of relaxation processes,[15] energy dissipation eventually heats the bulk sample, leading to a small but observable blue shift of the OH stretching

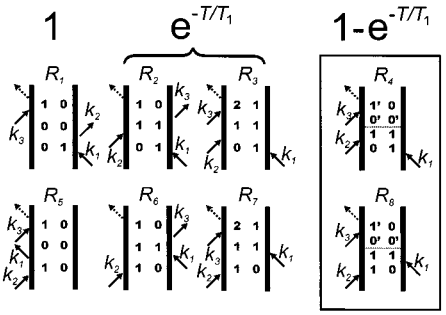

Figure 6. Double sided Feynman graphs which have to be considered. The upper row (R_1-R_4) describe the echo generating (rephasing) Liouville space pathways, while in the lower row R_5-R_8 symbolize the pathways, which do not generate an echo (nonrephasing). R_1, R_2, R_5, and R_6 are the diagrams for a two level system; R_3 and R_7 are also contributing in a three level system with excited-state absorption from $\nu = 1$ to $\nu = 2$. R_4 and R_8 take the process of relaxation to a "hot" ground state into account (see text for details). This process is symbolized by a horizontal dashed line. Above the diagrams are the multiplicative factors that are used for the response functions represented by the diagrams below. R_1 and R_5 do not decay because there is no relaxation channel feeding back population into $\nu = 0$. R_2, R_3, R_6, and R_7 decay with the population relaxation time T_1 since they describe pathways in which the system is in the $\nu = 1$ state during the population period T. Simultaneously the "hot" ground state $\nu = 0'$ is populated. Hence, the response functions R_4 and R_8 are multiplied by a factor of $1 - \exp(-T/T_1)$.

mode.[18] Hence, part of the spatial grating, which has initially been written into the sample by the first two laser pulses, remains for a very long time scale, which is limited only by thermal diffusion over macroscopic distances. This grating gives rise to the constant offset in the transient grating signal which does not decay on the time scales investigated and which is in fact a thermal grating (at least at long enough delay times).

We take into account this spectroscopic response by an extended level scheme (see Figure 5), where T_1 relaxation leads into a "hot", blue-shifted ground state rather than into the initially pumped ground state. As a consequence, the bleach is not refilled by population relaxation, while the excited state still decays with $\exp(-T/T_1)$. In addition, an absorption signal between the $\nu = 0' \rightarrow \nu = 1'$ level pair is obtained, which grows in by $1 - \exp(-T/T_1)$ (see Figure 5).

This has important consequences for the observation of inhomogeneous broadening and spectral diffusion, an information which is stored in the form of a frequency grating written by the first two laser pulses. Such a grating exists for both the bleach and the excited-state signal, and hence, both contain identical information about inhomogeneous broadening. When both sets of diagrams would decay simultaneously with population relaxation, as in the traditional two-level picture, observation of spectral diffusion processes would be limited to a time scale on the order of T_1. However, in the present case, the ground-state diagrams survive vibrational relaxation and allow spectral diffusion to be observed over an essentially infinite time range.

The essential idea of this model is the same as the traditional picture of hole burning, except that it happens on a much faster time scale. At low enough temperatures and in glasses, transient holes can be observed for 10^3 s and even longer,[19] even though the lifetime of the transitions under investigation is certainly much shorter (on the order of 1 ns). The important point is that the excited molecules do not specifically refill the hole after relaxation, but end up with random transition frequency. In a photon echo experiment, the first two light pulses burn a frequency grating into the absorption band rather than a hole (see Figure 7). Nevertheless, spectral diffusion will destroy this grating in exactly the same way as it destroys the hole in a hole-burning experiment.

4.1. Response Functions. In the following we present a self-contained model in the framework of Liouville space formalism[20] that includes the effect discussed in the previous section. We shall see that with this model we can predict the excitation wavelength dependence of the peak shift as well as the transient grating decay traces. Since the $\nu = 1 \rightarrow \nu = 2$ and the $\nu = 0 \rightarrow \nu = 1$ transitions are both resonant with the light field when the anharmonicity of the oscillator is sufficiently small, a vibrator has to be treated as a three-level system. The "conventional" response functions of a three-level system (see Feynman diagrams R_1-R_3 and R_5-R_7 in Figure 6) have been reported recently,[6] and are listed below with the corresponding decay factors:

$$R_1 = \mu_{01}^4 e^{-i\omega_{01}(t-\tau)} \exp[-g(\tau) + g(T) - g(t) - g(T+\tau) - g(t+T) + g(t+T+\tau)]$$

$$R_2 = e^{-T/T_1}\mu_{01}^4 e^{-i\omega_{01}(t-\tau)} \exp[-g(\tau) + g(T) - g(t) - g(T+\tau) - g(t+T) + g(t+T+\tau)]$$

$$R_3 = -e^{-T/T_1}\mu_{01}^2\mu_{12}^2 e^{i\alpha t} e^{-i\omega_{01}(t-\tau)} \exp[-g(\tau) + g(T) - g(t) - g(T+\tau) - g(t+T) + g(t+T+\tau)]$$

$$R_5 = \mu_{01}^4 e^{-i\omega_{01}(t+\tau)} \exp[-g(\tau) - g(T) - g(t) + g(T+\tau) + g(t+T) - g(t+T+\tau)]$$

$$R_6 = e^{-T/T_1}\mu_{01}^4 e^{-i\omega_{01}(t+\tau)} \exp[-g(\tau) - g(T) - g(t) + g(T+\tau) + g(t+T) - g(t+T+\tau)]$$

$$R_7 = -e^{-T/T_1}\mu_{01}^2\mu_{12}^2 e^{i\alpha t} e^{-i\omega_{01}(t+\tau)} \exp[-g(\tau) - g(T) - g(t) + g(T+\tau) + g(t+T) - g(t+T+\tau)] \quad (1)$$

The coupling to the thermal bath is incorporated by the line shape function $g(t)$

$$g(t) = \int_0^t d\tau_1 \int_0^{\tau_1} d\tau_2 \langle \delta\omega_{01}(\tau_2)\delta\omega_{01}(0)\rangle \quad (2)$$

and $\delta\omega_{01}(t)$ describes the fluctuating part of the transition frequency $\omega_{01}(t) = \omega_{01} + \delta\omega_{01}(t)$, and ω_{01} is the mean transition frequency $\langle\omega_{01}(t)\rangle$. μ_{01} and α are the transition dipole moment and the anharmonicity, respectively, which is defined as the difference between the $\nu = 1 \rightarrow \nu = 2$ and the $\nu = 0 \rightarrow \nu = 1$ transition frequency. It is assumed that the fluctuations $\delta\omega_{01}$ and $\delta\omega_{12}$ are strictly correlated ($\delta\omega_{01} = \delta\omega_{12}$) which implies that the solvent induced fluctuations of the potential surface affect only the harmonic term. For the transition dipole moments a harmonic approximation yielding $2\mu_{01}^2 = \mu_{12}^2$ is used. Since the anharmonicity $\alpha = \langle w_{01}(t)\rangle - \langle w_{12}(t)\rangle$ in liquid water is 270 cm^{-1},[21] which is much larger than the bandwidth of the laser pulses ($100 cm^{-1}$) these pathways have only a minor effect on the signal as we verified in numerical simulations.

In the extended level scheme Figure 5, additional Feynman diagrams R_4 and R_8 grow in, which describe the absorption between the $\nu = 0' \rightarrow \nu = 1'$ level pair. In the following, we will discuss two limiting cases and compare them with the experimental results: (A) The frequency memory is totally lost during relaxation of the excited state or (B) it is retained, as depicted schematically in Figure 7. In case A we have no correlation between $\nu = 0 \rightarrow \nu = 1$ and the $\nu = 0' \rightarrow \nu = 1'$

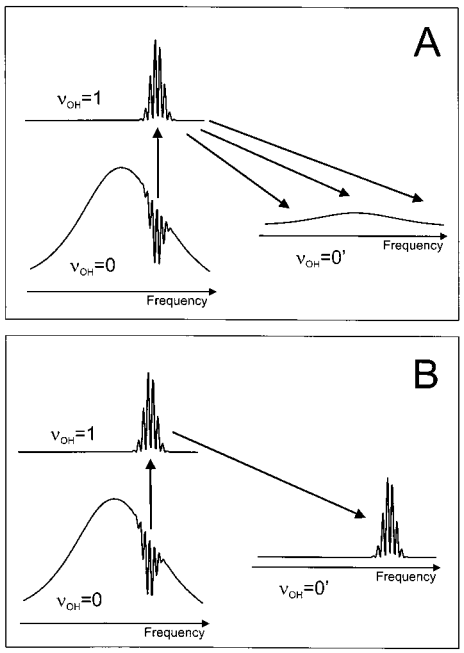

Figure 7. By the first two pulses interacting with the sample a frequency grating is burned into the ground state ($\nu = 0$) absorption band. Simultaneously a frequency grating appears in the excited state $\nu = 1$. During the process of population relaxation of the excited-state frequency grating to the "hot" ground state the memory of the original spectral position might be lost (case A) or conserved (case B).

absorption, and the response functions R_4 and R_8 are

$$R_4^{\text{uncorr}} = -(1 - e^{-T/T_1})\mu_{01}^2\mu_{0'1}^2 e^{i\omega_{01}(t-\tau)}e^{-i\Delta\omega t}e^{-g(\tau)}e^{-g(t)}$$

$$R_8^{\text{uncorr}} = -(1 - e^{-T/T_1})\mu_{01}^2\mu_{0'1}^2 e^{i\omega_{01}(t+\tau)}e^{-i\Delta\omega t}e^{-g(\tau)}e^{-g(t)} \quad (3)$$

where $\Delta\omega$ is the blue shift of the "hot" ground-state absorption $\nu = 0' \rightarrow \nu = 1'$ with respect to the original transition $\nu = 0 \rightarrow \nu = 1$. The transition dipole moments are assumed to be identical ($\mu_{01} = \mu_{0'1'}$). The response functions R_4^{uncorr} and R_8^{uncorr} enter the total response with a negative sign because there is only one interaction on the right (bra) side of the Feynman diagram.[20]

The pathways R_4^{uncorr} and R_8^{uncorr} can each be seen as a combination of two successive independent linear processes since the phase memory is assumed to be lost by relaxation to the hot ground state. Therefore the response functions reduce to a product of two two-point dipole correlation functions instead of a single 4-point dipole correlation function (eq 7.14 in ref 20). To obtain an intuitive picture of this situation, one can use a simple Bloch line shape function $g(t) = t/T_2 + {}^1/_2\Delta_{\text{inhom}}^2 t^2$. The response functions R_1 and R_2 are in this case proportional to $\exp(-\Delta_{\text{inhom}}^2(\tau - t)^2)$ while $R_4^{\text{uncorr}} \propto \exp(-\Delta_{\text{inhom}}^2\tau - \Delta_{\text{inhom}}^2 t)$. For a given τ in the first case the signal will peak at $t = \tau$. In other words, it forms a photon echo. In the latter case the maximum is always located at $t = 0$, not forming an echo at all.

Given this model, one can qualitatively understand the rise of the peak shift after vibrational relaxation of the system. The bleach (R_1) and "hot" ground state (R_4) signals have opposite signs and strongly tend to cancel each other (they would completely cancel when there would be no blue shift). As a function of time t, this cancellation is complete for that part of the bleach signal which does not contain frequency memory, i.e., the free induction decay which is emitted at $t = 0$ and decays quickly. The photon echo part of R_1, however, which is emitted later at $t = \tau$, is not canceled since the R_4 response function has nothing to oppose to. Hence, for large enough τ, the remaining signal will increase, giving rise to a large peak shift.

For the case of complete correlation between $\nu = 0 \rightarrow \nu = 1$ and $\nu = 0' \rightarrow \nu = 1'$ absorption (case B, see Figure 7) the response functions R_4^{corr} and R_4^{uncorr} are the same as R_1 and R_5, except for a frequency shift of $\Delta\omega$ and the transition dipole moments, which are however again assumed to be identical ($\mu_{01} = \mu_{0'1'}$).

$$R_4^{\text{corr}} = -(1 - e^{-T/T_1})\mu_{01}^2\mu_{0'1'}^2 e^{-i\Delta\omega t}e^{i\omega_{01}(t-\tau)}\exp[-g(\tau) + g(T) - g(t) - g(T+\tau) - g(t+T) + g(t+T+\tau)]$$

$$R_8^{\text{corr}} = -(1 - e^{-T/T_1})\mu_{01}^2\mu_{0'1'}^2 e^{-i\Delta\omega t}e^{-i\omega_{01}(t+\tau)}\exp[-g(\tau) - g(T) - g(t) + g(T+\tau) + g(t+T) - g(t+T+\tau)] \quad (4)$$

The detector measures the time-integrated square of the third-order polarization:

$$S(T,\tau) = \int_0^\infty |P^{(3)}(\tau,T,t)|^2\,dt \quad (5)$$

where the third-order polarization is obtained by convolution of the response functions R_j with the electric fields of the laser pulses:

$$P^{(3)}(\tau,T,t) = \int_0^\infty dt' \int_0^\infty dT' \int_0^\infty d\tau' \times \sum_j R_j(\tau',T',t')E_3(t-t')e^{-i\omega(t-t')}E_2(t-t'-T') \times e^{-i\omega(t-t'-T')}E_1(t-t'-T'-\tau')e^{+i\omega(t-t'-T-\tau')} \quad (6)$$

$E_{1,2,3}$ are the envelopes, and ω is the carrier frequency, of the three laser pulses.

4.2. Model Calculations. In this section we present illustrative calculations using the formalism described above (eqs 1−6) using models for the frequency correlation function, which are increasingly more complicated, but also increasingly more realistic. We follow this approach to gain an understanding of how the vibrational relaxation in a hydrogen bonded system influences the peak shift behavior and what can be learned about the frequency correlation function. We will compare both limiting cases A and B, which assume complete loss of all frequency memory after relaxation into the "hot" ground state and complete conservation of the memory, respectively (Figure 7). In the numerical calculations, we use the actual experimental pulse duration of 150 fs and the known parameters of the OH stretch transition of HDO in D_2O ($T_1 = 700$ fs,[2,22] $T_2 = 90$ fs,[3] $\alpha = 270$ cm^{-1} [21]).

Before exploring the effect of the relaxation to the "hot" ground state on the signal we perform first numerical simulations using the "conventional" model[6] that involves only levels $\nu = 0$, $\nu = 1$, and $\nu = 2$. In this case, vibrationally excited molecules relax to the original ground state $\nu = 0$. Figure 8 shows the peak shifts (D, E, and F) and transient gratings (G, H, and J) for different frequency correlation functions (A, B, and C). These model functions are described in detail later on and are presented here for direct comparison with the following calculations. In all cases the peak shift decays monotonically in a similar manner as the correlation function. The transient grating intensity decays monoexponentially with a time constant close to $T_1/2$ and exhibits no offset. These results are not in agreement with our experimental data and show that this model does not apply for the case of water.

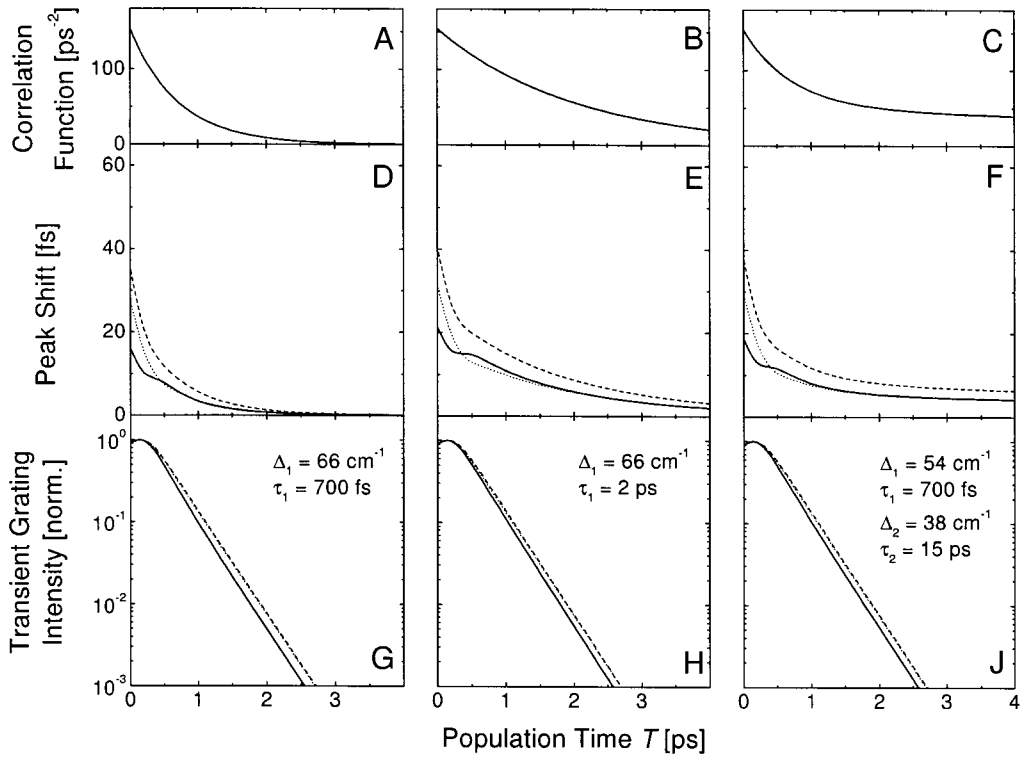

Figure 8. Calculation of the signals observed in an echo experiment using the 'conventional' level scheme with vibrational states $\nu = 0$, $\nu = 1$, and $\nu = 2$. On the top row the assumed correlation functions are shown according to eq 8 (A and B) and eq 9 (C), respectively. The corresponding calculated peak shift traces (D, E, and F) as well as the transient grating intensities (G, H, and J) are plotted for laser pulses centered at 3300 cm^{-1} (solid), 3400 cm^{-1} (dashed), and 3500 cm^{-1} (dotted).

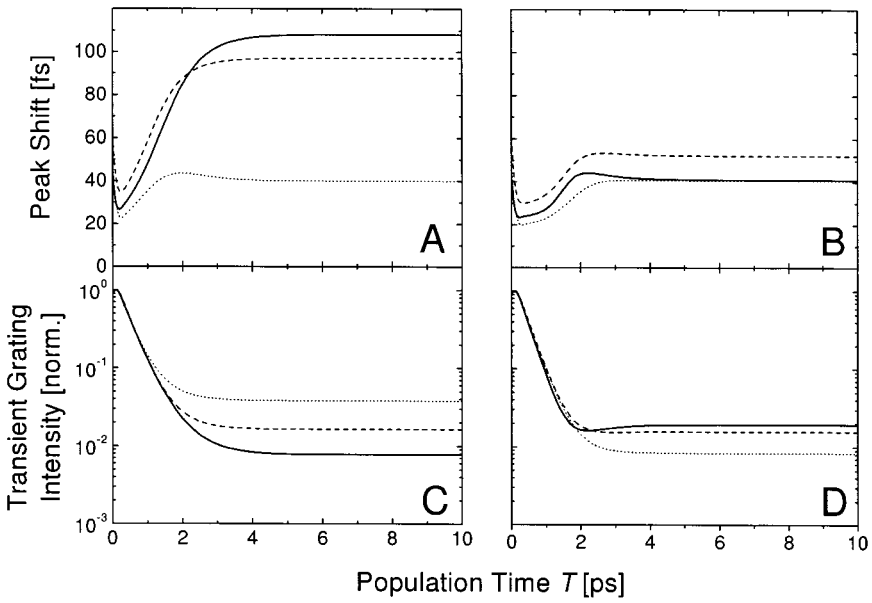

Figure 9. The calculated peak shift (A and B) and transient grating (C and D) using a Bloch model (eq 7) for laser pulses centered at 3300 cm^{-1} (solid), 3400 cm^{-1} (dashed), and 3500 cm^{-1} (dotted). On the left side (A and C) a total loss of frequency memory during population relaxation is assumed ($R_4 = R_4^{\text{uncorr}}$) while on the right (B and D) frequency memory is conserved ($R_4 = R_4^{\text{corr}}$). The enhancement of the peak shift upon population relaxation to the "hot" ground state is much stronger in the uncorrelated case (A) than in the correlated case (B).

Moving on to the more sophisticated approach with the extended level scheme (Figure 5), we determine in a first step the blue shift $\Delta\omega$ of the "hot" ground state. The blue shift is due to heating of the bulk solution and gives rise to a thermal grating for long enough population times T. Since the bleach signal and the $\nu = 0' \rightarrow \nu = 1'$ absorption signal tend to cancel each other (they would completely cancel when the blue shift would be zero), the long-time off-set of the transient grating signal does critically depend on the amount of the blue shift. Hence, by comparing the experimental off-set (see Figure 4B) with the numerical result (see Figures 9−11), we can estimate for the blue shift $\Delta\omega \approx 20 \pm 5$ cm^{-1}. Since the blue shift is a thermal effect, the long-time offset in the transient grating signal does not depend critically on the particular dephasing model used (Figure 9, Figure 10, or Figure 11), and we use the same value for $\Delta\omega$ for all model calculations. When a value is used beyond those given by the error ± 5 cm^{-1}, we see a significant discrepancy between experimental and calculated off-set values

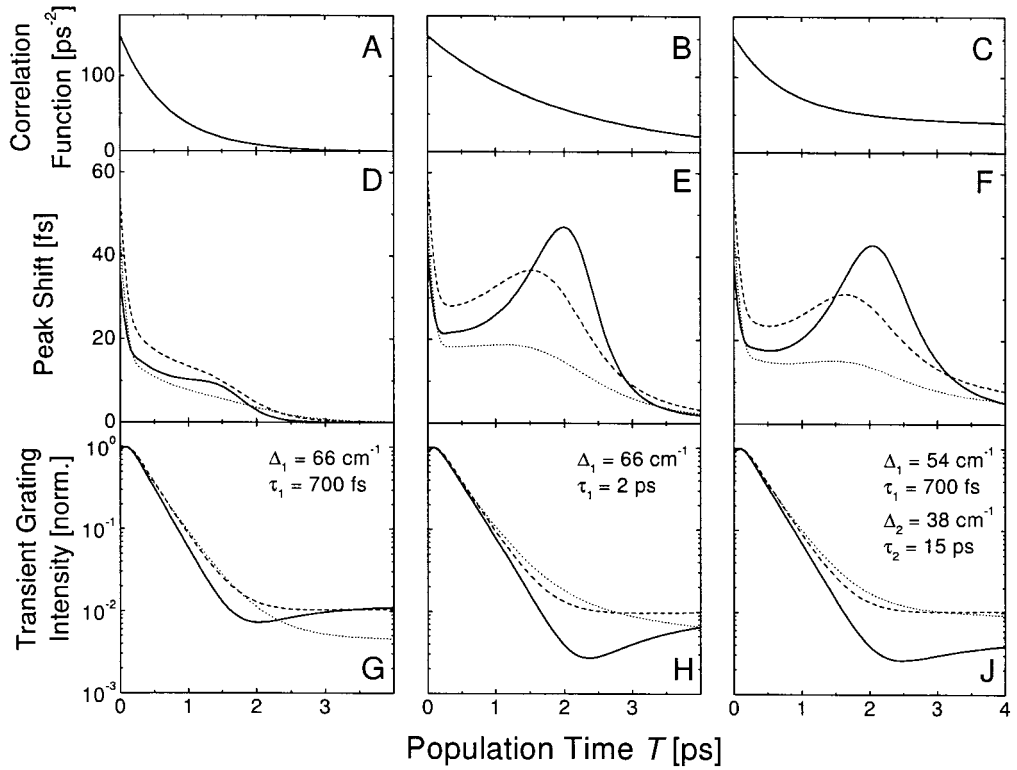

Figure 10. Simulation of the echo experiment with a Kubo model and assuming complete loss of frequency memory during population relaxation. On the top row the assumed correlation functions are shown according to eq 8 (A and B) and eq 9 (C), respectively. The corresponding calculated peak shift traces (D, E, and F) as well as the transient grating intensities (G, H, and J) are plotted for laser pulses centered at 3300 cm^{-1}(solid), 3400 cm^{-1} (dashed), and 3500 cm^{-1} (dotted). The calculations illustrated in the middle and the right column agree well with the experimental data.

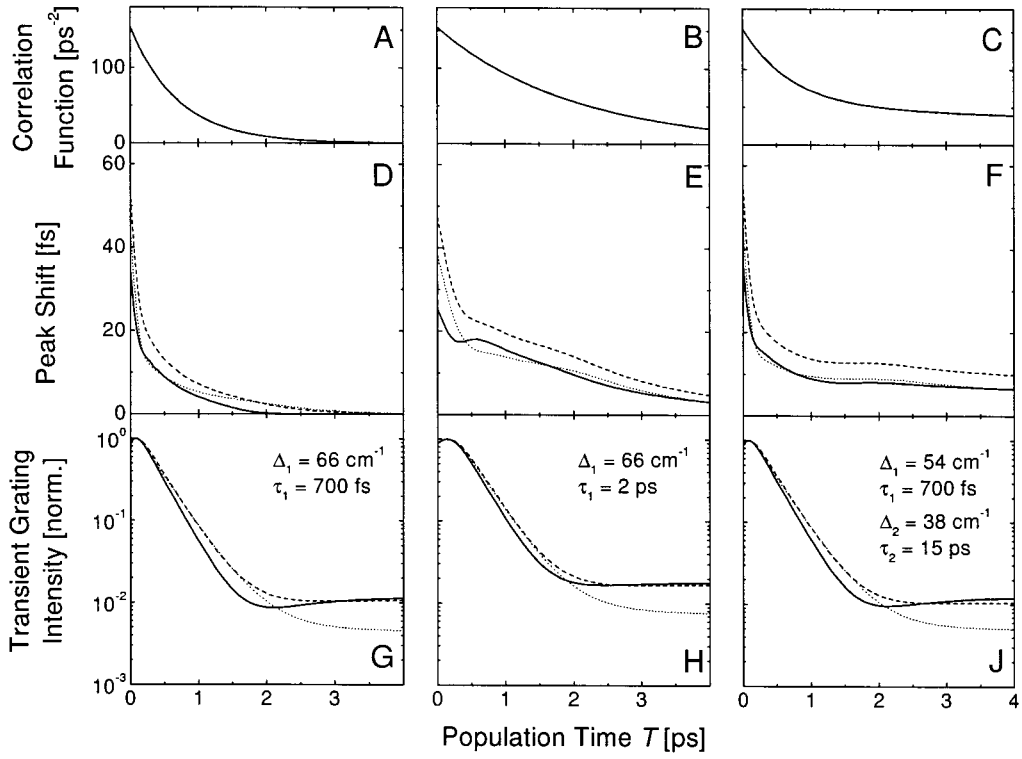

Figure 11. Simulation of the echo experiment with a Kubo model and assuming complete conservation of frequency memory during population relaxation. On the top row the applied correlation functions are shown using eq 8 (A and B) and eq 9 (C). The corresponding calculated peak shift traces (D, E, and F) as well as the transient grating intensities (G, H, and J) are plotted for laser pulses centered at 3300 cm^{-1} (solid), 3400 cm^{-1} (dashed), and 3500 cm^{-1} (dotted). No parameter set could be found to approximately reproduce the experimental observations.

of the transient grating signals. It should be noted that the blue shift of 20 cm^{-1} is consistent with the temperature-dependent shift observed in steady-state absorption spectroscopy.[23]

The most simple model for system bath interactions is the Bloch model that assumes a strict separation of time scales between ultrafast fluctuations giving rise to homogeneous

broadening and quasi-static inhomogeneous broadening. The Bloch model excludes processes, such as spectral diffusion, a simplification which certainly is not valid for liquid water. Nevertheless, we use this model as a first simple example that is easy to interpret and to demonstrate the strong enhancement of the peak shift due to a relaxation to a "hot" ground state. In Figure 9A,B the calculated peak shift is plotted over population time T for both limiting cases $R_4 = R_4^{\text{uncorr}}$ and $R_4 = R_4^{\text{corr}}$. The solid, dashed, and dotted lines represent 100 cm^{-1} red detuning, no detuning, and 100 cm^{-1} blue detuning of the laser pulses with respect to the center of the absorption band, respectively. For this simulation we use a frequency correlation function

$$\langle \delta\omega_{01}(t)\delta\omega_{01}(0)\rangle = \delta(t)/T_2 + \Delta_{\text{inhom}}^2 \qquad (7)$$

where the parameters $T_2 = 90$ fs and $\Delta_{\text{inhom}} = 66$ cm^{-1} have been determined recently[3] to reproduce the slope of the photon echo signal as function of τ, the peak shift at $T = 0$, and the total width of the absorption spectrum. In all six transients we observe a fast initial decay for $T \leq 200$ fs which is due to a pulse duration effect and vanishes when delta pulses are used (not shown). On a time scale close to T_1 the peak shift then rises to reach a constant value. This value differs for the two cases $R_4 = R_4^{\text{uncorr}}$ and $R_4 = R_4^{\text{corr}}$. When all frequency memory is lost (case A, Figure 9A), the enhancement of the peak shift is much larger (up to a level of 100 fs) than that in the correlated case B (Figure 9B) where the increase is not as dramatic. In general, this indicates that in both cases the population relaxation triggers an increase of the peak shift. This enhancement can be correlated to the presence of molecules in the "hot" ground state generated on the time scale of the population relaxation process. Therefore, we conclude that the evolution of the peak shift does not reflect the frequency correlation function as long as population relaxation takes place. For long time delays, however, the peak shift is constant and does represent the correlation function, namely, a constant, used as input into the simulation.

Inhomogeneity is not static in the liquid phase, and in liquid water the existence of spectral diffusion has been reported recently.[2] In the following, we want to investigate on what time scales spectral diffusion in water occurs by comparing model calculations for different relaxation times with the experimental data. The recent observation of spectral diffusion in a single-exponential manner[2] suggests a frequency fluctuation correlation function of the form

$$\langle \delta\omega_{01}(t)\delta\omega_{01}(0)\rangle = \Delta_1^2 \mathrm{e}^{-t/\tau_1} + \delta(t)/T_2 \qquad (8)$$

The first term represents a Kubo line shape with modulation strength Δ_1 and a correlation time τ_1, convoluted with a Lorentzian line shape corresponding to homogeneous broadening with $T_2 = 90$ fs.[3] To be consistent with the full width of the absorption line, we find $\Delta_1 = 66$ cm^{-1}.[3] Figure 10D,G shows the photon echo peak shift and the transient grating decay for case A for a correlation time $\tau_1 = 700$ fs, which is the value that has been reported recently from transient hole-burning experiments[2] (see Figure 10A). The transient grating signal is not that much different from the experimental data but clearly the rise in the peak shift is not reproduced. All peak shift traces decay monotonically. For the correlated case (Figure 11D,G) the disagreement is even stronger and the characteristic dip in the red detuned transient grating trace is not appearent like in the uncorrelated case. Hence, eq 8 with $\tau_1 = 700$ fs is not consistent with the photon echo data.

As a next step we varied the time constant in the Kubo term in eq 8, but kept all other parameters constant. We find that for $\tau_1 = 2$ ps in the uncorrelated case (Figure 10B,E,H) the peak shift and as well the transient grating match the experimental data satisfactory. The amplitude of the peak in the red detuned peak shift trace and its position at $T = 2$ ps is well reproduced. The general trend to the blue side of the band exhibiting smaller peak shifts for longer time delays is also apparent. In the transient grating the off set for population times longer than 4 ps is close to the experimental value of $\sim 10^{-2}$ and the dip in the red trace (solid line) at 2 ps is reproduced remarkably well. In contrast the calculation with the same parameters but $R_4 = R_4^{\text{corr}}$ do not give a good representation of the measurement (Figure 11B,E,H). No rise in the peak shift or a dip in the transient grating is present. In fact by varying τ_1 we could not find a time for which these features would be obtained.

Finally, we tried a multiexponential decay of the frequency fluctuation correlation function with two Kubo terms:

$$\langle \delta\omega_{10}(t)\delta\omega_{10}(0)\rangle = \Delta_1^2 \mathrm{e}^{-t/\tau_1} + \Delta_2^2 \mathrm{e}^{-t/\tau_2} + \delta(t)/T_2 \qquad (9)$$

With $\tau_1 = 700$ fs, $\Delta_1 = 54$ cm^{-1}, $\tau_2 = 15$ ps, and $\Delta_2 = 38$ cm^{-1} (Figure 10C,F,J) one achieves for case A a similarly good agreement with the experiment as with the single-exponential correlation function with $\tau_1 = 2$ ps. This is not surprising, because the correlation functions (Figure 10B,C) are very similar in the time region between 1 and 4 ps. In other words, the parameters are highly correlated and in fact we can obtain an equal match for a shorter correlation time τ_2 with a correspondingly larger amplitude Δ_2. In that sense, we cannot deduce from our experiment the exact functional form of the frequency fluctuation correlation function. Nevertheless, the existence of a peak shift at population times $T \geq 4$ ps shows that the frequency fluctuation correlation function has not completely decayed yet. As before, the correlated case B cannot describe the experimental result (see Figure 11C,F,J).

To summarize this paragraph, we have seen that we can qualitatively reproduce the features observed in the experimental data. However, we can conclude that they can be reproduced only when (a) we assume a rather long-lived component in the frequency fluctuation correlation function and (b) when we assume that frequency memory in the "hot" product state is essentially destroyed after relaxation. We have seen in Figure 9 that the destructive interference of several contribution to the total signal results in a dramatic increase of the peak shift, which rises on the time scale of population of the hot product state. However, since the frequency fluctuation correlation function decays, the peak shift eventually decreases for large enough population time T. Hence, two counteracting effects contribute to the size of the peak shift, resulting in a maximum at around 2 ps.

5. Discussion

Even though a photon echo peak shift experiment and a transient hole-burning experiment[2] are both capable to resolve inhomogeneous broadening and measure spectral diffusion processes,[20] and hence should reveal identical results, both experimental techniques are sensitive to different aspects of the complex relaxation process. For example, the photon echo experiment is a background free technique which allows to follow spectral diffusion processes for long time scales where the signal gets extremely small. On the other hand, integration over the signal (eq 5) destroys part of the information, so that interpretation of the signal at early delay times, where both spectral diffusion and population relaxation contribute simultaneously, is not straightforward. Thus, we conclude that the

transient hole-burning experiment is well suited to determine fast spectral diffusion processes, while the photon echo experiment is the method of choice for longer time scales.

We have seen from the model calculations that a single-exponentially decaying frequency fluctuation correlation function with a correlation time of $\tau_1 = 700$ fs cannot explain the experimentally observed photon echo peak shift. Even though the photon echo peak shift does not directly resemble the frequency fluctuation correlation function, such as it does in simple two-level systems,[7,8] the existence of a peak shift at times T around 2−4 ps nevertheless unambiguously proves that the frequency fluctuation correlation function has not yet completely decayed. Apparently, the hole-burning experiment in ref 2 missed that slow tail of the frequency fluctuation correlation function because the signal was too small. On the other hand, a single-exponentially decaying frequency fluctuation correlation function with a correlation time of $\tau_1 = 2$ ps, which would be consistent with our photon echo experiment, would probably not be consistent with the hole-burning result. We therefore conclude that the decay of the frequency fluctuation correlation function is nonexponential, with a fast component in the range of 700 fs and a slower component in the range of 5−15 ps (see Figure 10C,F).

Such a nonexponential decay with a rather slow tail is to be expected since there are numerous experimental observations which give strong evidence that water forms relatively stable, ice-like, structures. These include transient hole-burning experiments with longer pulses,[4] a slow component in the orientational relaxation of the OH dipoles in D_2O measured with the help of the anisotropy decay,[5] the Debye relaxation, which also measures orientational relaxation,[12,24,25] and results from NMR measurements.[26] As inhomogenenous broadening is in some complicated way related to the heterogeneous surrounding of the individual HDO molecules, structural diffusion will give rise to spectral diffusion, and the time scales of both processes are correlated. Hence, our experiment is yet another proof of the existence of long-lived structures in water, and it unites observations made before using different experimental techniques.

It is interesting to compare our results with molecular dynamics simulations. Diraison et al.[27] find for the system H_2O in D_2O that the frequency correlation function of the three vibrational normal modes can be mimicked using a biexponential expression with two time constants, 50 and 800 fs. As pointed out already in ref 27, the signatures of the fast response observed in ultrafast experiments depend strongly on the pulse duration. A correlation time as fast as 50 fs cannot be determined in our experiment with the current time resolution. We have recently published the two-pulse photon echo experiment on HOD/D_2O[3] where for the analysis we have assumed that for this fast process the fast modulation limit is valid with a resulting exponential decaying behavior for the O−H stretch with a T_2 value of 90 fs. This value represents an upper limit for fastest solvent fluctuation time scale. The 50 fs component in the MD result might well be responsible for this ultrafast coherence decay. The 800 fs component in the calculated response function of Diraison et al. agrees approximately with the 700 fs component used in our analysis of the experimental peak shift data. As noted by Bratos et al.[28] this value is also close to the hydrogen bond lifetime reported by Marti et al.[29] and Luzar/Chandler.[30] This suggests that they represent the same underlying mechanism. Simulations on the 5−15 ps time scale have not been realized in full extension. Therefore we hope that our findings on this long time scale will stimulate further theoretical work.

Furthermore, our model calculations verify that any frequency memory is completely lost after relaxation into the "hot" ground state, and only case A can describe the experimental data. For longer population times T this can readily be understood: As the blue shift of the $\nu = 0' \rightarrow \nu = 1'$ absorption band is a thermal effect, it averages over many molecules and the frequency memory about those molecules which had initially been excited (i.e. the hole) and which had dissipated the energy is completely lost. However, there is a second process which might explain a memory loss even for earlier times T where thermal diffusion is not completed. Energy relaxation from the OH vibration will initially excite (thermally or nonthermally) the immediate surrounding of the molecule, i.e., the hydrogen bonds which fix the molecule. Since the lifetime of these hydrogen bonds is only a few ps at room temperature, it seems reasonable that it is even shorter at the elevated high temperature which will be present for a short period of time. In other words, it seems likely that the structures fixing the OHD molecule are destroyed, leaving the molecule in a new, randomized surrounding. As the absorption frequency of the molecule is related to the surrounding, the absorption frequency will be randomized as well immediately after relaxation of the OH vibration.

6. Conclusions

In conclusion, we have presented the first photon echo peak shift study of the OH vibration of HDO dissolved in D_2O. Due to the strong anharmonic coupling of the OH vibration to its surrounding, the system cannot be treated as a simple two- or three-level system, because an extended model including a vibrationally "hot" ground state is required. We have presented a model which self-consistently describes the experimental data. The analysis shows that spectral diffusion, which is related to structural diffusion, exhibits a relatively slow tail which decays on a 5−15 ps time scale.

References and Notes

(1) Hadži, D.; Bratos, S. Vibrational spectroscopy of the hydrogen bond. In *The Hydrogen Bond: Recent Developments in Theory and Experiments*; Schuster, P., Zundel, G., Sandorfy, C., Eds.; North-Holland: Amsterdam, The Netherlands, 1976; Vol. II. Structure and Spectroscopy; pp 565−611.

(2) Gale, G. M.; Gallot, G.; Hache, F.; Lascoux, N. *Phys. Rev. Lett.* **1999**, *82*, 1068.

(3) Stenger, J.; Madsen, D.; Hamm, P.; Nibbering, E. T. J.; Elsaesser, T. *Phys. Rev. Lett.* **2001**, *87*, 027401.

(4) Laenen, R.; Rauscher, C.; Laubereau, A. *Phys. Rev. Lett.* **1998**, *80*, 2622.

(5) Woutersen, S.; Emmerichs, U.; Bakker, H. J. *Science* **1997**, *278*, 658.

(6) Hamm, P.; Lim, M.; Hochstrasser, R. M. *Phys. Rev. Lett.* **1998**, *81*, 5326.

(7) Joo, T.; Jia, Y.; Yu, J.-Y.; Lang, M. J.; Fleming, G. R. *J. Chem. Phys.* **1996**, *104*, 6089.

(8) de Boeij, W. P.; Pshenichnikov, M. S.; Wiersma, D. A. *Chem. Phys. Lett.* **1996**, *253*, 53.

(9) Passino, S. A.; Nagasawa, Y.; Joo, T.; Fleming, G. R. *J. Phys. Chem. A* **1997**, *101*, 725.

(10) Woutersen, S.; Bakker, H. J. *Nature* **1999**, *402*, 507

(11) Gale, G. M.; Gallot, G.; Lascoux, N. *Chem. Phys. Lett.* **1999**, *311*, 123.

(12) Rønne, C.; Åstrand, P.-O.; Keiding, S. R. *Phys. Rev. Lett.* **1999**, *82*, 2888.

(13) Yang, M.; Ohta, K.; Fleming, G. R. *J. Chem. Phys.* **1999**, *110*, 10243.

(14) Agarwal, R.; Krueger, B. P.; Scholes, G. D., Yang, M.; Yom, J.; Mets, L.; Fleming, G. R. *J. Phys. Chem. B* **2000**, *104*, 2908.

(15) Note that the relaxation channel depicted by the arrow in Figure 5 combines a complex sequence of relaxation steps including transient population of the OH and OD bending modes,[16] equilibration of the vibrational system,[18] and thermal diffusion. This crude simplification is justified by (i) the fast time scale of the whole sequence of processes[16,18] and (ii) by the fact that the photon echo giving rise to the peak shift behavior originates from the original bleach, and not the transient products.

(16) Deàk, J. C.; Rhea, S. T.; Iwaki, L. K.; Dlott, D. D. *J. Phys. Chem. A* **2000**, *104*, 4866.

(17) Rey, R.; Hynes, J. T. *J. Chem. Phys.* **1996**, *104*, 2356.

(18) Lock, A. J.; Woutersen, S.; Bakker, H. J. *J. Phys. Chem. A* **2001**, *105*, 1238.

(19) Koedijk, J. M. A.; Wannemacher, R.; Silbey, R. J.; Völker, S. *J. Phys. Chem.* **1996**, *100*, 19945.

(20) Mukamel, S. *Principles of Nonlinear Optical Spectroscopy*; Oxford University Press: New York, 1995.

(21) Graener, H.; Seifert, G.; Laubereau, A. *Phys. Rev. Lett.* **1991**, *66*, 2092.

(22) Woutersen, S.; Emmerichs, U.; Nienhuys, H.-K.; Bakker, H. J. *Phys. Rev. Lett.* **1998**, *81*, 1106.

(23) Iwata, T.; Koshoubu, J.; Jin, C.; Okubo, Y. *Appl. Spectrosc.* **1997**, *51*, 1269.

(24) Agmon, N. *J. Phys. Chem.* **1995**, *100*, 1072.

(25) Kaatze, U. *Chem. Phys. Lett.* **1993**, *203*, 1.

(26) Fung, B. M.; McGaughy, T. W. *J. Chem. Phys.* **1976**, *65*, 2970.

(27) Diraison, M.; Guissani, Y.; Leicknam, J.-Cl.; Bratos, S. *Chem. Phys. Lett.* **1996**, *258*, 348.

(28) Bratos, S.; Gale, G. M.; Gallot, G.; Hache, F.; Lascoux, N.; Leicknam, J.-Cl. *Phys. Rev. E* **2000**, *61*, 5211.

(29) Marti, J.; Padro, J. A.; Guardia, E. *J. Chem. Phys.* **1996**, *105*, 639.

(30) Luzar, A.; Chandler, D. *Nature* **1996**, *379*, 55.